17th World Conference on Earthquake Engineering, 17WCEE
Sendai, Japan - September 13th to 18th 2020

Prediction of the Peak Displacement of the Reinforced Concrete Structure with Brittle Members Based on the Momentary Energy Input

K. Fujii[(1)], H. Kanno[(2)], T. Nishida[(3)]

[(1)] *Professor, Chiba Institute of Technology, kenji.fujii@it-chiba.ac.jp*
[(2)] *Associate Professor, Akita Prefectural University, kanno@akita-pu.ac.jp*
[(3)] *Professor, Akita Prefectural University, tetsuya_nishida@akita-pu.ac.jp*

Abstract

It is widely accepted that the prediction of peak displacement for a given seismic intensity is one of the most important processes for the rational seismic evaluation of existing buildings and the seismic design of new buildings. Several studies have proposed methods, such as the capacity spectrum method (equivalent linearization technique), displacement coefficient methods, and the momentary energy input method. Most of these methods can be applied to ductile structures with good accuracy. However, few methods can be applied to structures with brittle members. Previous studies have reported that the nonlinear response of structures with brittle members is more significantly influenced by the ground motion characteristics. Specifically, the influence of sudden strength loss in brittle members to the peak response is more pronounced in the case of long-duration ground motions than in the case of short-duration ground motions. Therefore, the accuracy of the predicted peak response for brittle structures can be improved by considering the duration of input ground motion.

The concept of momentary energy input has been proposed by Inoue et al. to predict the peak response of ductile reinforced concrete (RC) structures. The basic idea of the momentary energy input method is to equate the maximum momentary input energy to the sum of cumulative hysteresis energy and damping energy per half cycle. Because this method can easily consider the shape of the hysteresis loop, the method can be extended to structures with brittle members. To this end, the authors investigated the relationship of the maximum moment energy input with the duration of ground motions. Subsequently, the authors formulated the time-varying function of the momentary input energy using a Fourier series for an elastic single-degree-of-freedom (SDOF) model. Using the time-varying function of the momentary input energy, the peak response of a structure with brittle members can be more accurately predicted by considering the duration of input ground motion.

In this study, the peak displacement of the RC structures with brittle members was predicted using the concept of momentary energy input. The proposed method is outlined as follows:

1. Calculate the cumulative strain energy of the structure until the displacement at brittle failure, E_{su}.
2. Calculate the time-varying function of the momentary energy input of the elastic SDOF model with consideration to the effective period of the structure corresponding to the displacement at brittle failure. Then, calculate the cumulative energy input up to the maximum momentary energy input, $E_{I\,pre}$.
3. From the ratio of E_{su} and $E_{I\,pre}$, assess whether brittle failure occurs up to the maximum momentary energy input. If the ratio $E_{I\,pre}/E_{su}$ exceeds the limit value, the peak response can be evaluated by considering only the ductile member. Otherwise, it can be evaluated by considering the brittle and ductile members. The process of predicting the peak response is carried out using the momentary energy input method.

The numerical results revealed that the peak response of a structure with brittle members can be satisfactorily predicted for short- and long-duration ground motions using the proposed method.

Keywords: Momentary Input Energy, Brittle Member, Reinforced Concrete Structure, Fourier Phase Angle

1. Introduction

In earthquake-prone countries, such as Japan, there are still many reinforced concrete (RC) buildings with insufficient seismic capacity against extreme seismic excitations. Most of these buildings, which are not designed to satisfy the current (updated) seismic design code, consist of brittle and ductile members. Therefore, to evaluate the seismic capacity of these buildings, it is important to consider the strength loss of brittle members (for example, columns and walls with low shear reinforcements and infills) to predict if the nonlinear response is an important issue.

Nowadays, the existing simplified nonlinear analysis procedures, which combine the nonlinear static (pushover) analysis of a multi-degree-of-freedom (MDOF) model with the response spectrum analysis of an equivalent single-degree-of-freedom (SDOF) model, have been widely implemented in the seismic evaluation guidelines of existing buildings [1–4]. To better predict the seismic peak response of an existing building with brittle members, the authors have previously conducted investigations using nonlinear static analysis [5]. In a previous study, it was found that the accuracy of the equivalent linearization technique strongly depends on the characteristics of ground motions, even though these ground motions are generated to fit the same spectrum. In other words, in the case of long-duration ground motions, the energy absorption of brittle members should be ignored when predicting the peak response. However, this is overly conservative in the case of short-duration ground motions. Even though the inelastic response spectrum has been proposed for structures with brittle members (infilled RC frames) [6], there are currently no methods considering the influence of the duration of ground motions for predicting the peak response of RC structures with brittle members.

Inoue et al. proposed the concept of momentary energy to predict the peak response of ductile RC structures [7-9]. The basic idea of the momentary energy input method is to equate the maximum momentary input energy to the sum of the cumulative hysteresis energy and damping energy per half cycle. Because this method can directly consider the shape of the hysteresis loop, it can be extended to structures with brittle members. Accordingly, the authors formulated a time-varying function of the momentary input energy using the Fourier series for an elastic SDOF model [10]. By using the time-varying function of the momentary input energy, the peak response of a structure with brittle members can be more accurately predicted by considering the duration of input ground motion.

In this study, the peak displacement of RC structures with brittle members was predicted using the concept of momentary energy input. In this study, the investigation was simplified by considering the case of an undamped SDOF model. The effect of viscous damping will be investigated in future work.

2. Prediction of peak displacement based on momentary input energy

2.1 Definition of momentary input energy

Considering the nonlinear response of a SDOF model without viscous damping, the equation of motions can be expressed as follows:

$$m\ddot{y}(t)+f_R(t)=-ma_g(t), \tag{1}$$

where m is the mass of the SDOF model, y and f_R are the displacement and restoring forces of the SDOF model, respectively, and a_g is the ground acceleration. In this study, the restoring force f_R was assumed to be the sum of the brittle and ductile members, f_{RS} and f_{RF}, respectively. According to Inoue et al. [7-9], the momentary input energy during a half cycle of the structural response (from t to $t+\Delta t$) is defined as follows:

$$\Delta E=-m\int_t^{t+\Delta t} a_g(t)\,\dot{y}(t)\,dt\,. \tag{2}$$

The maximum momentary input energy, ΔE_{max}, is defined as the maximum value of ΔE over the course of the seismic event. Figure 1 illustrates the definition of maximum momentary input energy. Figure 1(a) shows an example of a case wherein brittle failure occurred during a half cycle at the maximum momentary energy input, while Figure 1(b) shows an example of a case wherein brittle failure occurred before the maximum momentary energy input.

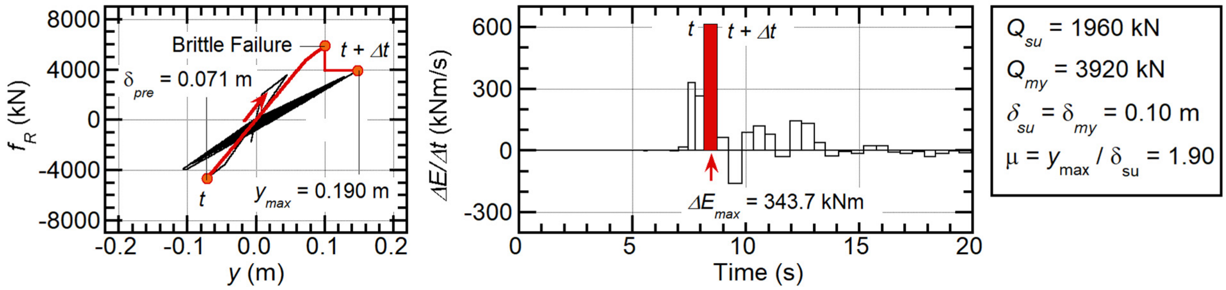

(a)

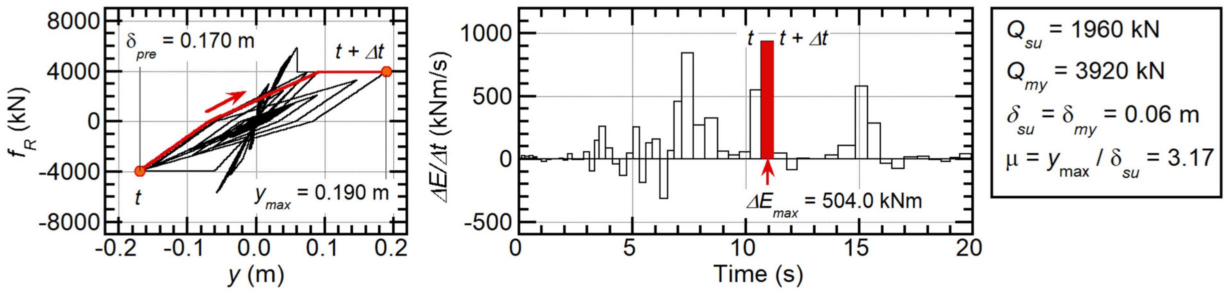

(b)

Fig. 1 – Definition of maximum momentary input energy. (a) Model: Cf04Cs02-H15, input ground motion: JKB-00 ($\alpha_1 = 1.00$); (b) model: Cf04Cs02-H09, input ground motion: TOH-00 ($\alpha_1 = 0.85$).

The equivalent velocity of the maximum momentary input energy $V_{\Delta E}$ is defined as follows:

$$V_{\Delta E} = \sqrt{2\Delta E_{\max} / m}\,. \tag{3}$$

2.2 Time-varying function of maximum momentary input energy

In this study, two seismic intensity parameters were used to predict the peak response of a structure with brittle members. One parameter is the maximum momentary input energy $\Delta E_{\max}$, and the other one is the cumulative energy input up to the maximum momentary energy input, E_{Ipre}. If E_{Ipre} is larger than the cumulative strain energy limit until brittle failure occurs (E_{su}), it is assumed that brittle failure occurs before the time of maximum momentary energy input. For the calculation of both $\Delta E_{\max}$ and E_{Ipre}, the time-varying function of momentary input energy formulated by the authors in a previous study [10] was used. The discrete time history of ground acceleration $a_g(t)$, defined within the range $[0, t_d]$, can be expressed using a Fourier series, as follows:

$$a_g(t) = \sum_{n=-N}^{N} c_n \exp(i\omega_n t)\,. \tag{4}$$

In Eq. (4), c_n and ω_n are the complex Fourier coefficient of the ground acceleration and the circular frequency of the n^{th} harmonic, respectively. Additionally, it is assumed that c_0 is equal to zero. As discussed in a previous paper [10], the time-varying function of the momentary input energy is expressed as follows:

$$\frac{1}{\Delta t}\frac{\Delta E(t)}{m} \approx \frac{1}{\Delta t}\frac{\widehat{\Delta E}(t)}{m} = \sum_{n=-N+1}^{N-1} E_{\Delta,n}{}^{*} \exp(i\omega_n t), \tag{5}$$

$$\text{where } E_{\Delta,0}{}^{*} = E_0{}^{*}, E_{\Delta,n}{}^{*} = \frac{\sin(\omega_n \Delta t/2)}{\omega_n \Delta t/2} E_n{}^{*}, \tag{6}$$

$$E_n{}^{*} = \begin{cases} \sum_{n_1=n+1}^{N} \left\{ H_{CVV}(i\omega_{n_1}) + H_{CVV}(-i\omega_{n_1-n}) \right\} c_{n_1} c_{-(n_1-n)} & : 0 \le n \le N-1 \\ \overline{E_{-n}{}^{*}} & : -N+1 \le n \le -1 \end{cases}. \tag{7}$$

$$\Delta t \approx \frac{T'}{2} = \pi \sqrt{\sum_{n=1}^{N} \left| H_{CVD}(i\omega_n) \right|^2 \left| c_n \right|^2 \Big/ \sum_{n=1}^{N} \left| H_{CVV}(i\omega_n) \right|^2 \left| c_n \right|^2}, \tag{8}$$

Note that the bar over a symbol indicates a complex conjugate. In Eqs. (7) and (8), $H_{CVV}(i\omega_n)$ and $H_{CVD}(i\omega_n)$ are the velocity and displacement transfer function of the linear SDOF system with viscous and complex damping (natural circular frequency ω_0, viscous damping ratio h, and complex damping ratio β), which is defined as follows:

$$H_{CVV}(i\omega_n) = i\omega_n H_{CVD}(i\omega_n), H_{CVD}(i\omega_n) = \frac{1}{\omega_0{}^2 - \omega_n{}^2 + 2\omega_0 \left\{ h\omega_n + \beta\omega_0 \operatorname{sgn}(\omega_n) \right\} i}, \tag{9}$$

$$\text{where } \operatorname{sgn}(\omega_n) = \begin{cases} 1 & : \omega_n > 0 \\ -1 & : \omega_n < 0 \end{cases}. \tag{10}$$

The momentary input energy per unit mass at time t is calculated as follows:

$$\frac{\Delta E(t)}{m} \approx \int_{t-\Delta t/2}^{t+\Delta t/2} \frac{1}{\Delta t}\frac{\widehat{\Delta E}(t)}{m} dt = \int_{t-\Delta t/2}^{t+\Delta t/2} \sum_{n=-N+1}^{N-1} E_{\Delta,n}{}^{*} \exp(i\omega_n t) dt, \tag{11}$$

The cumulative input energy per unit mass from time 0 to t is calculated as follows:

$$\frac{E_I(t)}{m} \approx \int_0^t \sum_{n=-N+1}^{N-1} E_n{}^{*} \exp(i\omega_n t) dt. \tag{12}$$

The predicted maximum momentary input energy per unit mass, $\Delta E_{\max}/m$, is the maximum value obtained from Eq. (11) over the course of the seismic event, while the j^{th} local maximum value of Eq. (11) is expressed as ${}_j\Delta E/m$. Figure 2(a) shows the calculation of ${}_j\Delta E/m$ from Eq. (11).

Let $t_{\Delta Emax}$ be the time of the predicted maximum momentary input energy. The cumulative energy input until time t_{pre} ($t_{\Delta Emax} \le t_{pre} \le t_d - \Delta t / 2$), E_{Ipre}, is defined as follows:

$$E_{Ipre} = E_I(t_{pre}) - \frac{1}{2}\Delta E(t_{pre}). \tag{13}$$

For the calculation of E_{Ipre}, the time t_{pre} is defined as follows. Let ${}_J\Delta E$ be the last local value, which is larger than 50% of $\Delta E_{\max}$, as shown in Fig. 2(b). The time t_{pre} is defined as the time of the J^{th} local maximum of Eq. (11). Therefore, the energy E_{Ipre} is calculated as the blue area in Fig. 2(c).

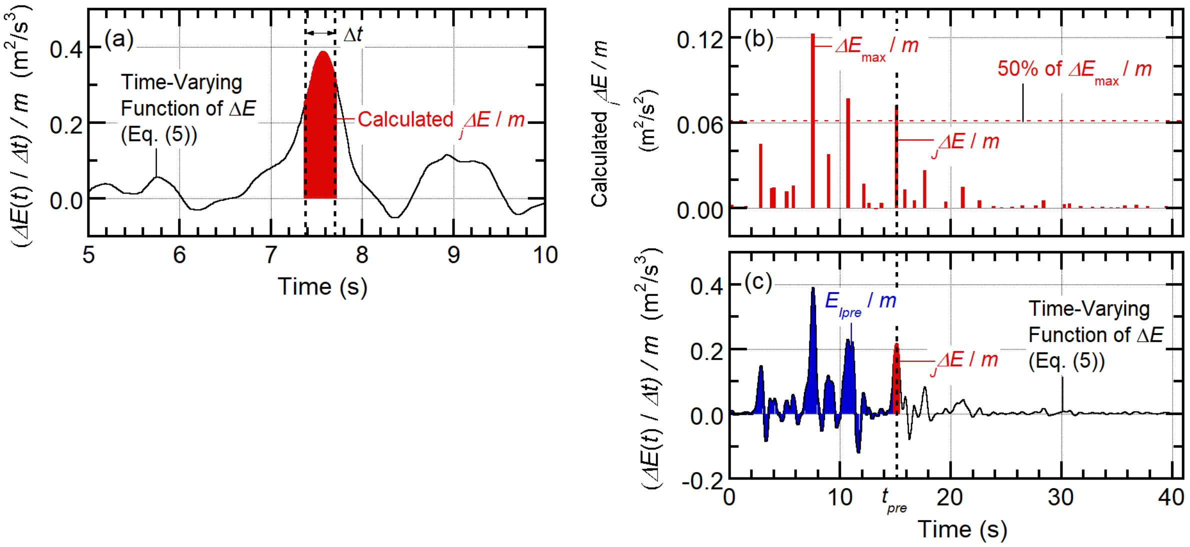

Fig. 2 – Calculation of ${}_nΔE$ and E_{Ipre} from time-varying function of $ΔE$: (a) calculation of ${}_nΔE$ per unit mass; (b) time history of ${}_nΔE$ per unit mass; (c) calculation of E_{Ipre} per unit mass.

If the time t_{pre} is taken as $t_{ΔEmax}$, Eq. (13) can be rewritten as follows:

$$E_{Ipre} = E_I\left(t_{\Delta E\max}\right) - \frac{1}{2}\Delta E\left(t_{\Delta E\max}\right) = E_I\left(t_{\Delta E\max}\right) - \frac{1}{2}\Delta E_{\max}\,. \tag{14}$$

Equation (14) is theoretically correct for calculating E_{Ipre} if the natural period of the considered structure is constant until brittle failure occurs. However, owing to the cracking of structural members, the natural period may vary from the initial failure until brittle failure. Therefore, Eqs. (13) and (14) are both considered in the prediction of peak response. This mater will be further discussed in later sections.

2.3 Description of proposed procedure

2.3.1 STEP 1: Calculation of SDOF model properties

The simplified restoring force–displacement (f_R-y) relationship and the properties of the SDOF model can be determined according to Figure 3(a). For simplification, the yield displacement of the ductile member, δ_{my}, is assumed to be the same as the displacement occurring at brittle failure, δ_{su}. Next, calculate the secant period at point SU and Y, T_{su}, and T_{my}, respectively, and the cumulative strain energy until δ_{su}, E_{su} (Figure 3(a)).

2.3.2 STEP 2: Assessment of brittle failure before maximum momentary energy input

Calculate the coefficient of the time-varying function of $ΔE$ (Eq. (5)) from Eqs. (6) through (10) for the linear SDOF model with a natural period T_{su} , h=0.10, and β=0.00. Then, calculate the cumulative energy input until the time t_{pre}, E_{Ipre}, from Eq. (13) (or. Eq. (14)), and compare the calculated E_{Ipre} with E_{su}. If $E_{su}>E_{Ipre}$, brittle failure does not occur before the $ΔE_{\max}$ inputs. Otherwise, brittle failure does occur before the $ΔE_{\max}$ inputs.

2.3.3 STEP 3: Prediction of peak displacement from energy balance in half cycle

(i) In the case of $E_{su}>E_{Ipre}$ (brittle failure does not occur before the $ΔE_{\max}$ inputs): calculate the peak displacement until the maximum momentary energy input, δ_{pre}, according to (i) in Figure 3(b). Then, calculate the effective period T_e and the dissipated hysteresis energy during a half cycle, $ΔE_\mu$, as the function of the peak displacement $y_{\max}$ ($y_{\max} \geq \delta_{pre}$).

(ii) In the case of $E_{su} \leq E_{Ipre}$ (brittle failure occurs before the $ΔE_{\max}$ inputs): calculate the effective period T_e and the dissipated hysteresis energy during a half cycle, $ΔE_\mu$, according to (ii) in Figure 3(b), as the function of peak displacement $y_{\max}$ ($y_{\max} \geq \delta_{my}$).

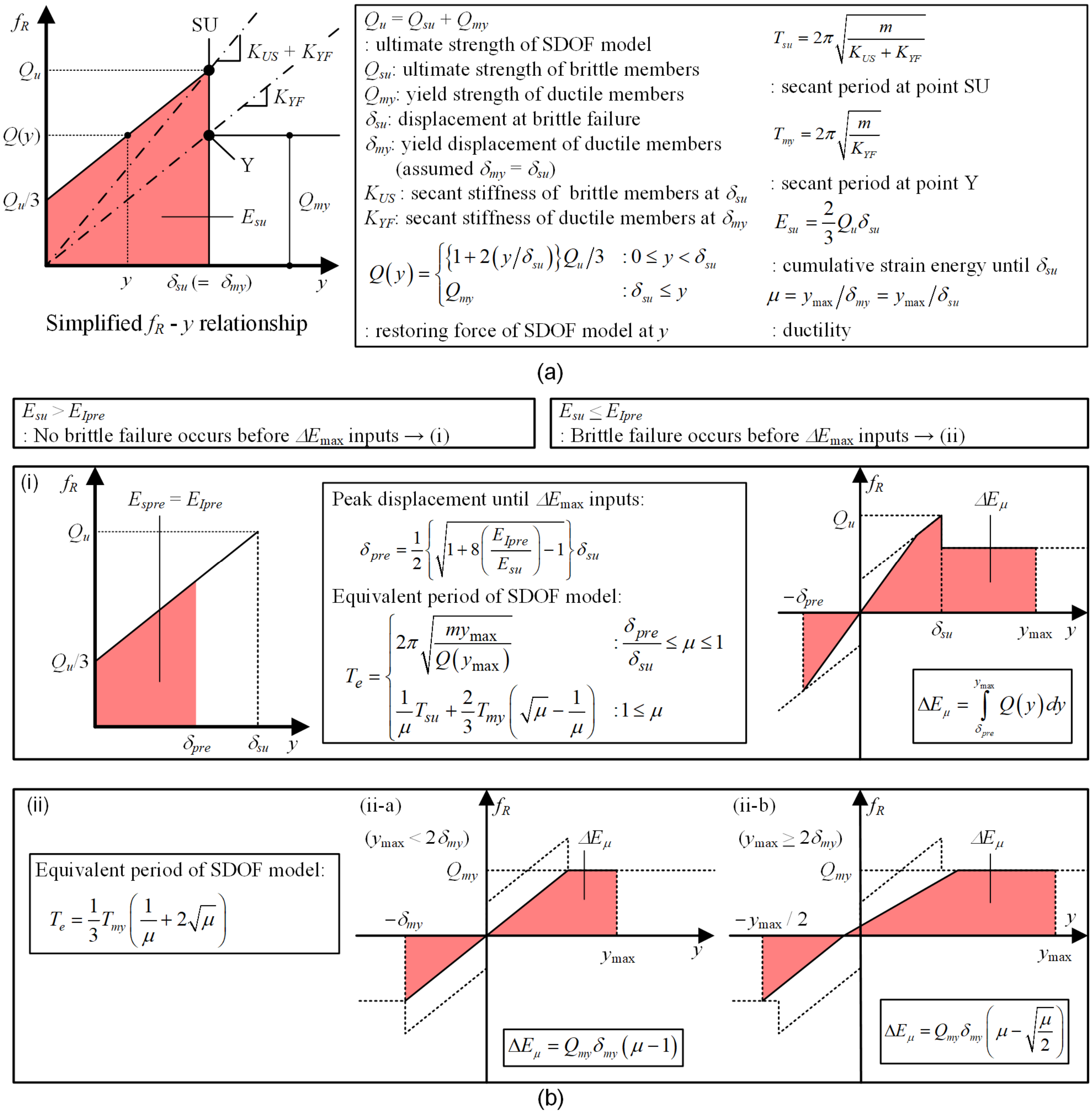

Fig. 3 – Definitions of simplified SDOF model properties: (a) simplified restoring force–displacement relationship; (b) equivalent period and dissipated hysteresis energy during half cycle.

Figure 4 shows the prediction of peak displacement using the maximum momentary input energy spectrum ($V_{\Delta E}$ spectrum). Using Eqs. (5)–(12), the maximum momentary input energy per unit mass, $\Delta E_{\max}/m$, for the linear SDOF model with a damping ratio h=0.10 and β=0.00 is calculated for each natural period T. The equivalent velocity $V_{\Delta E}$ can be calculated from the calculated $\Delta E_{\max}/m$ using Eq. (3).

The dissipated hysteresis energy during a half cycle, ΔE_μ, is also converted to the equivalent velocity $V_{\Delta E\mu}$, as follows:

$$V_{\Delta E\mu} = \sqrt{2\Delta E_\mu/m}\,. \tag{15}$$

The predicted response point is the intersection of the demand curve ($V_{\Delta E}$ spectrum) and capacity curve ($V_{\Delta E\mu}$-T_e relationship) shown in Figure 4(a) (point A or B). Then, the predicted peak displacement can be obtained as the value shown in Figure 4(b) (points A' and B').

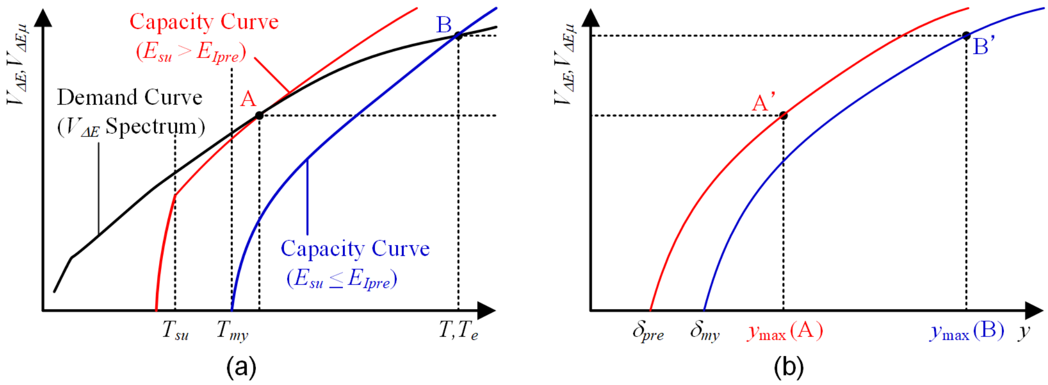

Fig. 4 – Prediction of peak displacement using $V_{\Delta E}$ spectrum.

3. Numerical analysis model and ground motion data

3.1 Numerical analysis model

The properties of the numerical models discussed in the following section are described as follows. The mass of the model m was assumed to be 1000 tons. The envelopes and hysteresis rules for the brittle and ductile RC members are shown in Fig. 5. The origin-oriented model (right part of Figure 5(a)) was used to model the hysteresis behavior of brittle members. To model the behavior of ductile members, the Muto hysteresis model [11] was used (right part of Figure 5(b)). Specifically, the unloading stiffness after yielding, K_{RF}, was proportionally decreased to $\mu^{-0.5}$ to represent the degradation of the unloading stiffness after the yielding of the RC members, in the same manner as in Otani's model [12].

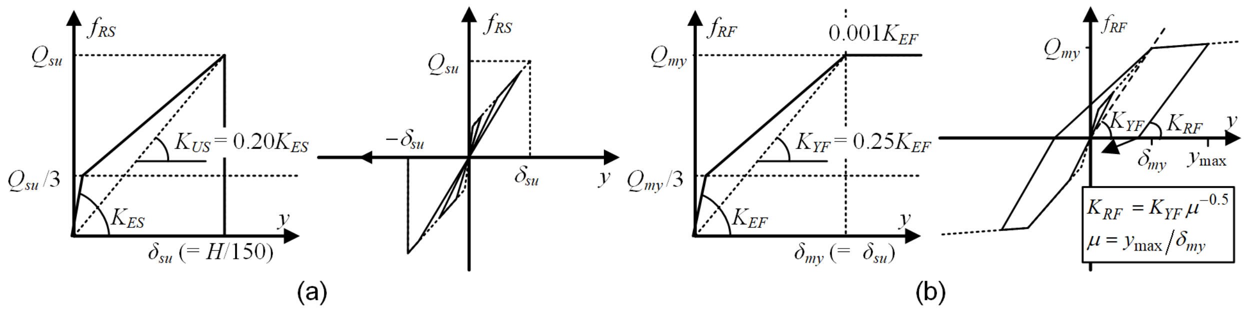

Fig. 5 – Envelopes and hysteresis rules for brittle and ductile RC members: (a) brittle members (dominated by shear behavior); (b) ductile members (dominated by flexural behavior).

In this study, the ultimate strength of the brittle members Q_{su} and the yield strength of the ductile members Q_{my} is defined as follows:

$$Q_{su} = C_s mg, Q_{my} = C_f mg, \tag{16}$$

where g is the gravitational acceleration, and C_s and C_f are the shear coefficient of the brittle and ductile members. In this study, the sum of C_s and C_f was set to 0.6 for all models. The height of the SDOF model, which is the parameter required to determine δ_{su}, was set to 9.0 m and 15.0 m. Table 1 lists the numerical models.

Table 1 – List of numerical models.

Model ID	C_f	C_s	H (m)	K_{EF} (MN/m)	K_{ES} (MN/m)	T_{su} (s)	T_{my} (s)	E_{su} (kNm)
Cf04Cs02-H09	0.4	0.2	9.0	261.3	163.3	0.635	0.777	235.2
Cf03Cs03-H09	0.3	0.3	9.0	196.0	245.0	0.635	0.898	235.2
Cf02Cs04-H09	0.2	0.4	9.0	130.7	326.7	0.635	1.099	235.2
Cf04Cs02-H15	0.4	0.2	15.0	156.8	98.0	0.819	1.004	392.0
Cf03Cs03-H15	0.3	0.3	15.0	117.6	147.0	0.819	1.159	392.0
Cf02Cs04-H15	0.2	0.4	15.0	78.4	196.0	0.819	1.419	392.0

3.2 Ground motions

In this study, 48 ground motions were generated from four recorded ground motions: the recorded motions used in this analysis are the horizontal major component of El Centro 1940 (ELC), Hachinohe 1968 (HAC) [13], JMA Kobe 1995 (JKB), and Tohoku University 1978 (TOH). Because there is unavoidable dispersion in the nonlinear time history analysis results, twelve semi-artificial ground motions are generated for each record by shifting the phase angle; the time history of the shifted ground acceleration $a_g(t, \Delta\varphi_0)$ is expressed as follows:

$$a_g\left(t, \Delta\varphi_0\right) = \sum_{n=-N}^{N} c_n \exp\left[i\left\{\omega_n t - \mathrm{sgn}\left(\omega_n\right)\Delta\varphi_0\right\}\right], \tag{17}$$

where $\Delta\varphi_0$ is the constant for shifting the phase angle of all harmonics. In this study, $\Delta\varphi_0$ was set from 0 to 11π/12 in π/12 intervals; the groups ELC (wave ELC-00 to ELC-11), HAC (wave HAC-00 to HAC-11), JKB (wave JKB-00 to JKB-11), and TOH (wave TOH-00 to TOH-11) were generated from each record.

Figure 6 shows the comparison of the $V_{\Delta E}$ spectrum (h=0.10) for each group. In this figure, "calculated $V_{\Delta E}$" was calculated using the time-varying function of ΔE (Eq. (11)), while "wave 00 to 11" was calculated from the linear time history analysis using each semi-artificial ground motion. As shown in the figure, the $V_{\Delta E}$ spectrum calculated from Eq. (11) is in good agreement with the spectra calculated from each semi-artificial ground motion.

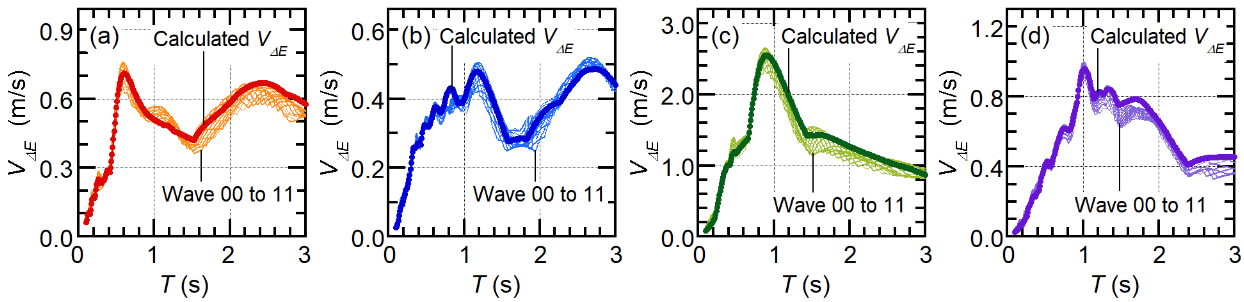

Fig. 6 – $V_{\Delta E}$ spectrum of unscaled input ground motions: (a) Group ELC; (b) group HAC; (c) group JKB; (d) group TOH.

In this study, the ground motions were scaled through multiplication with factor α, which is defined as follows:

$$\alpha = \alpha_0\alpha_1, \alpha_0 = \sqrt{\Delta E_{\max}\left(T_{su}\right)/E_{su}}\ . \tag{18}$$

where $\Delta E_{max}(T_{su})$ is the maximum momentary input energy of the linear SDOF model (natural period T_{su}, h=0.10, β=0.00) calculated using Eq. (11), α_0 is the scaling factor when $\Delta E_{max}(T_{su})$ is equal to E_{su}, and α_1 is the scaling factor normalized by α_0. In this study, factor α_1 was set to 0.70, 0.85, 1.00, 1.15, and 1.30 for all models. Therefore, the number of the nonlinear time history analyses was 6×5×4×12=1440.

4. Validation of proposed procedure

4.1 Prediction cases

Two cases were considered to validate the proposed procedure. In the first case (Case A), the maximum momentary input energy is the cumulative energy input up to the maximum momentary energy input, and E_{Ipre} is calculated from Eq. (14) under the assumption of $t_{pre}=t_{\Delta Emax}$. In the second case (Case B), E_{Ipre} is calculated from Eq.(13), assuming that the time t_{pre} is defined as the time of the J^{th} local maximum of Eq. (11), as shown in Figure 2(c) (the last local value, which is larger than 50% of ΔE_{max}).

4.2 Analysis results

Figure 7 compares the predicted peak displacement normalized by δ_{su} with that obtained from the nonlinear time history analysis results. In this figure, (a1) through (a3) are the results predicted by Case A, while (b1) through (b3) are the results predicted by Case B. As shown in Figure 7(a1) through (a3), the results predicted by Case A underestimated some results obtained from the nonlinear time history analysis. However, for case

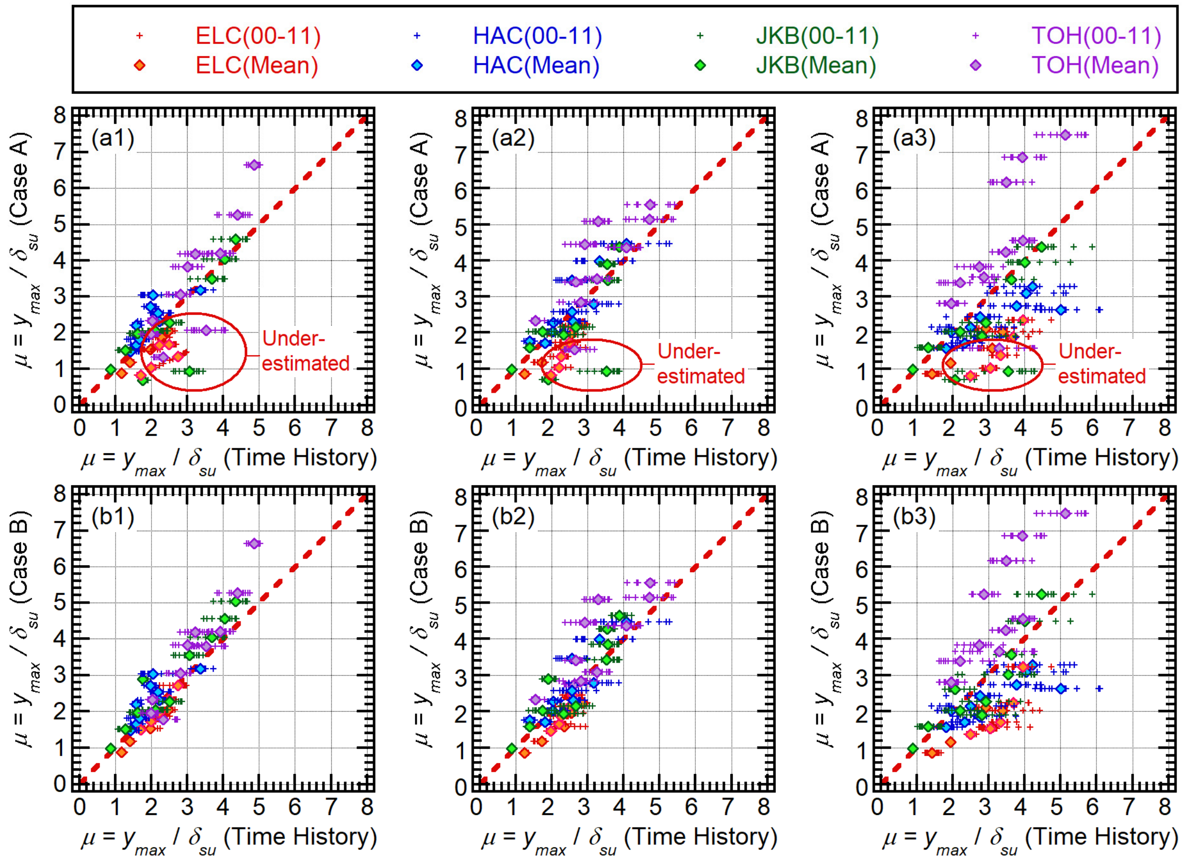

Fig. 7 – Accuracy of predicted peak response. (a1) C_f = 0.4, C_s = 0.2 (Case A); (a2) C_f = 0.3, C_s = 0.3 (Case A); (a3) C_f = 0.2, C_s = 0.4 (Case A); (b1) C_f = 0.4, C_s = 0.2 (Case B); (b2) C_f = 0.3, C_s = 0.3 (Case B); (b3) C_f = 0.2, C_s = 0.4 (Case B).

$C_f = 0.4$, $C_s = 0.2$ (Figure 7 (b1)) and case $C_f = C_s = 0.3$ (Figure 7 (b2)), the results predicted by Case B are in good agreement with the nonlinear time history analysis results. In the case of $C_f = 0.2$, $C_s = 0.4$, large scattering was observed as shown in Figure 7 (b3).

Based on the results shown in Figure 7, it can be concluded that the results predicted by Case B are in better agreement than those predicted by Case A. The proposed procedure (Case B) provides reliable results in the cases of $C_f = 0.4$, $C_s = 0.2$ and $C_f = 0.3$, $C_s = 0.3$, while in the case of $C_f = 0.2$, $C_s = 0.4$, large scattering was observed in the nonlinear time history analysis results. Therefore, based on the results obtained by this study, the proposed procedure may be applicable in the case wherein the yield strength of ductile members is larger than the ultimate strength of brittle members ($C_f > C_s$). Because larger scattering was observed in the nonlinear time history analysis results when $C_f < C_s$, it is concluded that the prediction of peak displacement is unreliable in such cases.

4.3 Discussion

To discuss the difference in the accuracy achieved in each of the two cases, the peak displacement until the maximum momentary energy input, δ_{pre}, was investigated according to each nonlinear time history analysis result. Figure 8 shows the relationship of δ_{pre}/δ_{su} and E_{Ipre}/E_{su}, calculated from the time-varying function of ΔE (Eq. (13) or (14)). Notably, the dotted curve equation is the simplified equation for calculating δ_{pre} from the ratio E_{Ipre}/E_{su}, as shown in Figure 3(b)).

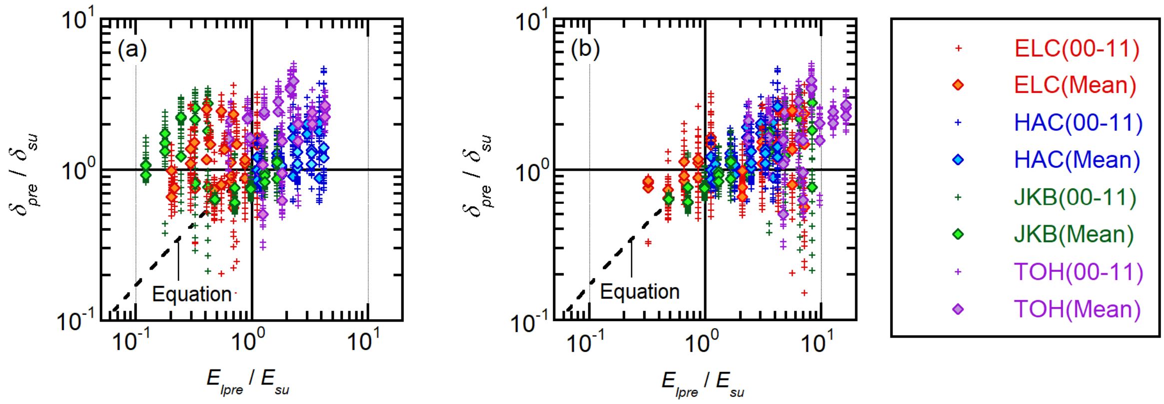

Fig. 8 – Relationship of δ_{pre}/δ_{su} (obtained from time history analysis) and E_{Ipre}/E_{su} calculated from the time-varying function of ΔE: (a) Case A (Eq. (14)); (b) Case B (Eq. (13)).

In Case A shown in Figure 8(a), there are some cases wherein the ratio $E_{Ipre}/E_{su}<1$ while $\delta_{pre}/\delta_{su}>1$. In such cases, the assessment of brittle failure is not conservative. In contrast, in Case B shown in Figure 8(b), the number of cases wherein $E_{Ipre}/E_{su}<1$ and $\delta_{pre}/\delta_{su}>1$ is smaller than that in Case A. Therefore, the assessment of brittle failure is more valid in Case B than in Case A.

Figure 9 compares the predicted t_{pre} at the time of maximum momentary energy input in the nonlinear time history analysis results. The case shown in this figure presents the results of Cf04Cs02-H09, and is shown in Figure 7(a1) as "underestimated". As can be seen, the time of the maximum momentary energy input was between the t_{pre} predicted in Case A and that predicted in Case B. In the case of JKB shown in Figure 9(a), the t_{pre} predicted in Cases A and B was 7.66 and 12.12 seconds, respectively, while the time of maximum momentary energy was between 8.52 to 11.3 seconds. Similar results were obtained for the TOH case shown in Figure 9(b). Therefore, the prediction of E_{Ipre} based on Eq. (14) ($t_{pre}=t_{\Delta E\max}$) is not conservative for any of the two cases.

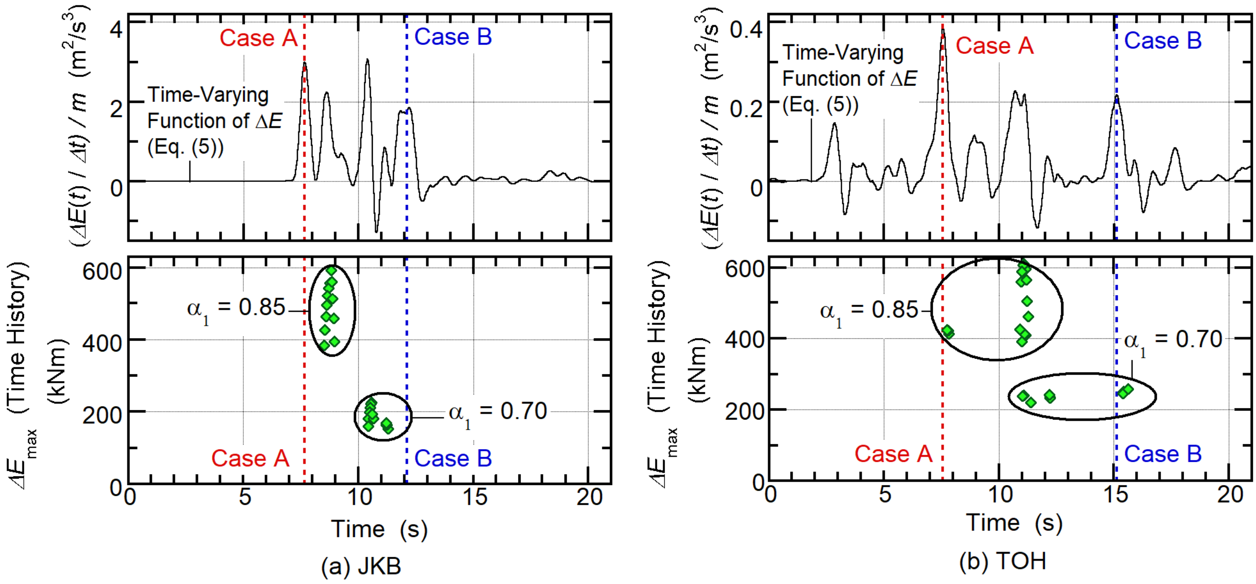

Fig. 9 – Comparisons of t_{pre} predicted from unscaled time-varying function of ΔE and time at $\Delta E_{\max}$ in time history analysis for model Cf04Cs02-H09: (a) JKB group; (b) TOH group.

5. Conclusions

In this study, the peak displacement of RC structures with brittle members was predicted using the concept of momentary energy input. The main contributions and results of this study are as follows.

(1) The predicted peak displacement is in good agreement with the nonlinear time history analysis results, provided that the cumulative energy input up to the maximum momentary energy input is properly predicted. To this end, the use of the time-varying function of the momentary input energy is useful.

(2) The proposed procedure may be applicable in the case wherein the yield strength of ductile members is larger than the ultimate strength of brittle members. In the case wherein the yield strength of ductile members was smaller than the ultimate strength of brittle members, larger scattering was observed in the nonlinear time history analysis results.

In this study, the investigations were simplified by considering the case of an undamped SDOF model. To extend this procedure such that it considers viscous damping, the following points must be investigated: (a) the cumulative viscous damping energy up to the maximum momentary energy input; (b) the dissipated viscous damping energy during a half cycle of the structural response. According to point (a), the time-varying function of relative velocity, which has been presented in a previous study [10], may be useful. Hence, by considering the proper combination of viscous damping and complex damping (representing the cumulative strain energy after cracking), the cumulative viscous damping energy may be predicted. Therefore, the cumulative strain energy (demand) can be estimated. For point (b), the dissipated viscous damping energy in a half cycle can be modelled as the dissipated hysteresis energy by considering the appropriate loop. These issues will be investigated in future work.

Acknowledgements

The ground motions used in this study were taken from the websites of the Japan Meteorological Agency (https://www.data.jma.go.jp/svd/eqev/data/kyoshin/index.htm, last accessed on 14 December 2019), and Building Performance Standardization Association (https://www.seinokyo.jp/jsh/top/, last accessed on 14 December 2019). We thank Edanz Group (https://en-author-services.edanzgroup.com/) for editing a draft of this manuscript.

References

[1] ATC-40. (1996): *Seismic Evaluation and Retrofit of Concrete Buildings*; Applied Technology Council: Redwood City, CA, USA.

[2] FEMA. (1997): *NEHRP Guidelines for the Seismic Rehabilitation of Buildings*; FEMA Publication 273; Federal Emergency Management Agency: Washington, DC, USA.

[3] CEN (2004): *Eurocode 8—Design of Structures for Earthquake Resistance. Part 1: General Rules, Seismic Actions and Rules for Buildings*; European standard EN 1998-1; European Committee for Standardization: Brussels, Belgium.

[4] ASCE (2017): *Seismic Evaluation and Retrofit of Existing Buildings*; ASCE standard, ASCE/SEI41-17; American Society of Civil Engineering: Reston, VA, USA.

[5] Fujii K (2016): Accuracy of predicted peak response of existing middle-rise steel reinforced concrete building using equivalent linearization technique, *Journal of Structural and Construction Engineering*, *Transactions of the AIJ*, **81**(721): 483-493. (in Japanese).

[6] Dolsek M, Fajfar P (2004): Inelastic spectra for infilled reinforced concrete frames, *Earthquake Engineering & Structural Dynamics*, **33** (15): 1395-1416.

[7] Nakamura T, Hori N, Inoue N (1998): Evaluation of damaging properties of ground motions and estimation of maximum displacement based on momentary input energy, *Journal of Structural and Construction Engineering*, *Transactions of the AIJ*, **513**: 65-72. (in Japanese).

[8] Inoue N, Wenliuhan H, Kanno H, Hori N, Ogawa J (2000): Shaking Table Tests of Reinforced Concrete Columns Subjected to Simulated Input Motions with Different Time Durations, *12th World Conference on Earthquake Engineering*, 30 January – 4 February, Auckland, New Zealand.

[9] Hori N, Inoue N (2002): Damaging properties of ground motion and prediction of maximum response of structures based on momentary energy input. *Earthquake Engineering & Structural Dynamics*, **31** (9): 1657-1679.

[10] Fujii K, Kanno H, Nishida T (2019): Formulation of the Time-Varying Function of Momentary Energy Input to a SDOF System by Fourier Series, *Journal of Japan Association for Earthquake Engineering*, **19** (5):247-266. (in Japanese).

[11] Muto K, Hisada T, Tsugawa T, Bessho S (1974): Earthquake resistant design of a 20 story reinforced concrete buildings, *5th World Conference on Earthquake Engineering*. 25-29, June, Rome, Italy.

[12] Otani S (1981): Hysteresis models of reinforced concrete for earthquake response analysis. *J Faculty of Engineering*, University of Tokyo, **36**(2): 125-156.

[13] Midorikawa S, Miura H (2010): Re-digitization of Strong Motion Accelerogram at Hachinohe Harbor during the 1968 Tokachi-oki, Japan Earthquake, *Journal of Japan Association for Earthquake Engineering*, **10** (2): 12-21. (in Japanese)

